Small Scale Fading Characteristics of Wideband Radio Channel in the U-shape Cutting of High-speed Railway

Lei Tian[†], Jianhua Zhang[*†], Chun Pan[†],
[*]Key Laboratory of Universal Wireless Communications (Beijing Univ.of Posts and Telecom.), Ministry of Education, China
Email: jhzhang@bupt.edu.cn
[†]Wireless Technology Innovation Institute, Beijing Univ. of Posts and Telecom., P.O. box #92, China,100876
Email: tianlbupt@bupt.edu.cn, panchun1987@gmail.com

***Abstract*—High-speed railway (HSR), as an important deployment scenario for both the present and the future mobile wideband radio communication systems, has attracted more and more attention all over the world with the rapid increasing demand of the high data rate communication service on traveling. For the purpose of capturing the wideband channel characteristics of HSR, a channel measurement campaign was conducted at the center frequency of 2.35 GHz with 50 MHz bandwith in the U-shape cutting scenario of Zhengzhou–Xian HSR line in China. Based on the field measured data, we analyze the small scale characteristics in detail, which maily include path number, root mean square delay spread (rms DS), and doppler shift. It is found that the distribution of the path number is well fitted by a Gamma distribution. The statistics of rms DS in the U-shape cutting scenario are larger than the results in other scenario of HSR. In addition, an increasing tendency of rms DS against the transmitter-to-receiver distance is observed and can be modeled by a linear function. Finally, the doppler frequency shift is verified and meets the theoretical value.**

I. Introduction

In recent years, high-speed railway (HSR) in China has developed rapidly after the great success in many other countries like Germany, France and Japan, etc., the total mileage of which has ranked No. 1 in the world according to the statistics by July 2012. Meanwhile, the 3rd generation mobile radio communication system, which has been widely deployed over the world, is providing communication services with higher data rate and wider bandwidth than before. Supporting the high data rate and wideband transmission has already become not only a tendency but also a basic requirement for the development of the future communication technologies. Therefore, to meet the increasing demand of the communication services on HSR, the mobile radio communication technologies need to be upgraded urgently to support the high data rate and wideband in the high-speed mobility environment.

The knowledge of the channel characteristics, as the prerequisite of the research of communication technologies, is of great important. And the channel measurement is the most direct and effective way to capture the channel characteristics. However, to the best of the author's knowledge, the measurement campaigns of the wideband channel for HSR are extremely insufficient. The studies on HSR channel characteristics in most published literatures are based on the narrow band system measurements like the global system for mobile communication - railway (GSM-R) system [1], [2]. Due to the restrictions of the equipment and fund, only a few wideband field channel measurement campaigns of HSR were carried out. [3] has reported a wideband HSR channel measurement campaign at 5 GHz with 125 MHz bandwidth by using RUSK sounder of Medav in Germany. Besides, two measurement campaigns were conducted at 2.35 GHz in the viaduct scenario of HSR by using Elektrobit Propsound$^{\mathrm{TM}}$ CS channel sounder [4] in Beijing and Taiwan of China, respectively [5], [6].

In addition, the scenarios of HSR with their own characteristics are quite different from those of the traditional cellular network, which include viaduct, U-shape cutting, plain, and tunnel, etc. Those scenarios should be investigated separately. Taking the U-shape cutting scenario for instance, the existing literatures mainly focus on the large scale fading characteristics like path loss and Ricean K-factor [2], [7]. Rare analysis is proceeded on the small scale fading characteristics like root mean square delay spread (rms DS) and path number. Only [8] presents relative complete measurement results on rms DS, max delay and path number in the U-shape cutting scenario based on the measurement at a center frequency of 2.1 GHz with 3.84 MHz bandwidth. Therefore, we perform a wideband channel measurement campaign at a center frequency of 2.35 GHz with 50 MHz bandwidth for the purpose of capturing the wideband channel characteristics in the HSR U-shape cutting scenario. For a further step, the statistical characteristics of path number, rms DS and doppler effect are analyzed in detail.

The remainder of the paper is organized as follows. Firstly, the channel sounding system and the measurement environment are described in Section II. Subsequently in Section III, the detailed processing procedure of the measured data is explained. Then the results of the concerned channel characteristics are analyzed in Section IV. Finally, conclusions are drawn in Section V.

TABLE I
PARAMETERS OF SYSTEM CONFIGURATION.

Items	Settings
Center frequency	2.35 GHz
Chip rate	25 MHz
Signal sampling rate	50 MHz
PN code length	127
Transmitting power at antenna input	33 dBm
Channel sampling rate	1968.504 Hz

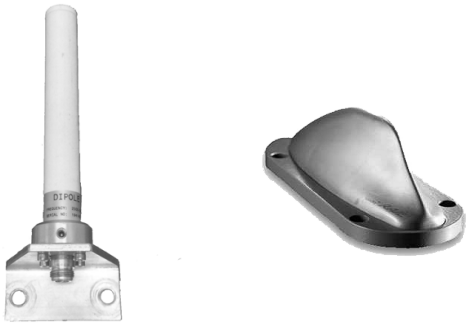

(a) VDP (b) HUBER+SUHNER

Fig. 1. The features of antennas used at (a) TX and (b) RX.

II. CHANNEL MEASUREMENT CHAMPAIGN

A. Measurement System and Antennas

The channel measurement campaign was carried out in the U-shape cutting of Zhengzhou–Xian HSR line in China at the center frequency of 2.35 GHz with 50 MHz bandwidth by using Elektrobit $\mathrm{Propsound}^{\mathrm{TM}}$ CS channel sounder. The clock signals of the transmitter (TX) and the receiver (RX) were synchronized by the global position system (GPS) during the measurement campaign. A pseudo-random (PN) sequence of 127 length was generated at the TX with a chip rate of 25 MHz. At the RX, the channel impulse response (CIR) were obtained by slide correlating the received signal with a synchronized copy of the sequence. A vertical-polarized dipole antenna was employed at the TX, as shown in Fig. 1(a). As for the RX, a train-mounted wideband vertical-polarized antenna HUBER+SUHNER [9] is used, the outfit of which is illustrated in Fig. 1(b). The parameters of the system configuration are summarized in Tab. I.

B. Measurement Environment

The measured environment is in the U-shape cutting of a typical rural area which is located at about 4 kilometers east to the Mount Hua North Station on the Zhangzhou–Xian HSR line. The U-shape cutting is characterized by the upper width of 40 meters, the bottom width of 16 meters and the depth of 8.85 meters. It is a deep U-shape cutting according to the definition given in [2]. A broad plain with scattered scrubby trees extends along the U-shape cutting. The TX antenna was fixed on a mast which is 5 meters high and about 20 meters away from the southern side of the U-shape cutting. The Rx antenna was mounted on the top of the high-speed train which traveled at a constant speed of about 200 km/h.

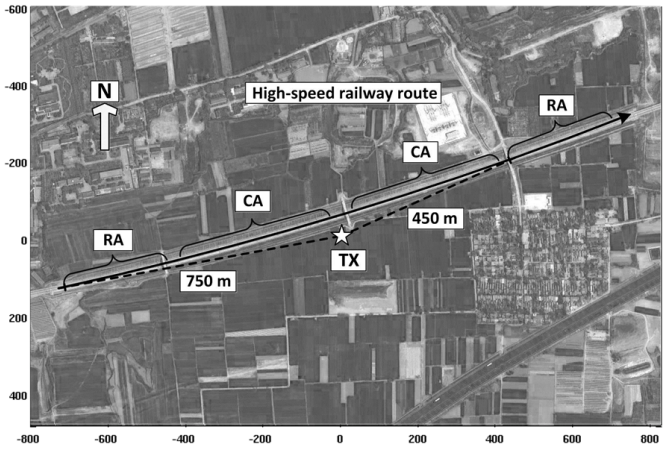

Fig. 2. Measurement route plan. The axis ticks are in 1 m.

The high-speed train travels from the west to the east in the U-shape cutting, illustrated as an arrow in Fig. 2. The length of the whole measured route is nearly 1500 meters. The TX was located near the middle of the route, which is marked by the star in Fig. 2. A line-of-sight (LOS) path exists between the TX and the RX in most part of the route except for the part obstructed by the overpasses across the U-shape cutting. There are three overpasses on the route. One is close to the TX location. The other two are both about 450 meters away to the west and to the east of the TX location, respectively. For the easy of the result analysis in the following, the label "WA" is utilized to identify the area of the whole measured route. The label "CA" is defined as the part with the TX-to-RX (T-R) distance range from 50 m to 400m, as shown in Fig. 2. In this area, the channel data are collected in a good LOS propagation condition without the effect of the overpass. And the part with the T-R distance range from 450 m to 750 m is labeled by "RA" in Fig 2, where the measured route is obstructed by the overpass more or less.

III. ESTIMATION OF SMALL SCALE PARAMETERS

A. Pre-definition

The measured channel impulse response (CIR) collected by the sliding correlation detector at time t_n can be modeled as $h(\tau_m, t_n), m = 1, \cdots, M$, where τ_m indicates the delay of the mth sample in the delay domain. M is the sampling length of a CIR snapshot at time t_n. Then the power delay profile corresponding to the CIR at time t_n can be calculated by

$$P(\tau_m, t_n) = \|h(\tau_m, t_n)\|^2, m = 1, \cdots, M., \qquad (1)$$

where$\|\cdot\|$ indicates 2-norm operation.

B. Path Number

The number of the paths of a CIR snapshot equals to the number of the extremum values of the power delay profile.

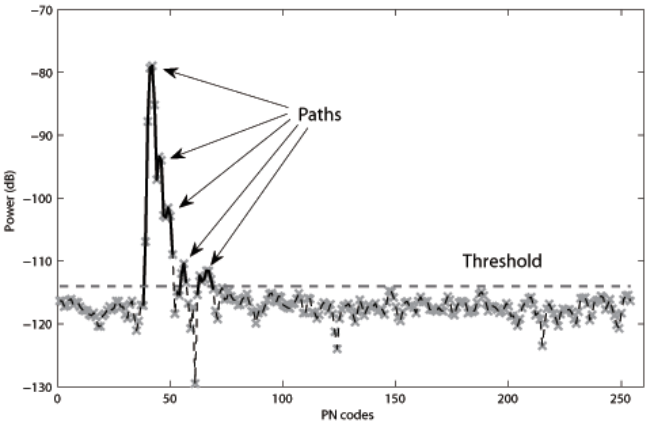

Fig. 3. Illustration of paths in a CIR snapshot.

Firstly, we define the sub-paths as a set of all the valid sampling values of the CIR snapshot. Based on the definition of the CIR before, the sub-path set of the CIR can be further defined by

$$\mathcal{A}_n = \{h(\tau_m, t_n) \,|\, P(\tau_m, t_n) > \mathrm{X}_n, m = 1, \cdots, M\}, \quad (2)$$

where X_n is a empirical threshold which is related to the noise level of the CIR. For ease of analysis, we define $\mathcal{U}_n = \{\tau_m \,|\, h(\tau_m, t_n) \in \mathcal{A}_n, m = 1, \cdots, M\}$. Then the extremum values set of the power delay profile can be denoted by

$$\begin{aligned} \mathcal{B}_n = \quad & \{P(\tau_m, t_n) \,|\, P(\tau_m, t_n) > P(\tau_{m-1}, t_n), \\ & P(\tau_m, t_n) > P(\tau_{m+1}, t_n), \tau_m \in \mathcal{U}_n\}. \end{aligned} \quad (3)$$

Thereby, the path number of the CIR is the element number of $\mathcal{B}_n$. For ease of understanding, an example of the paths of a CIR snapshot is illustrated in Fig. 3.

C. Delay Spread

The rms DS is defined as the root mean square of second central moment of the power delay profile [10]. So the rms DS sample of a certain CIR can be simply calculated by

$$\sigma_\tau(t_n) = \sqrt{\overline{\tau^2(t_n)} - \overline{\tau(t_n)}^2}, \quad (4)$$

where the bar over the variable means doing the average operation, $\overline{\tau^2(t_n)}$ and $\overline{\tau(t_n)}$ can be calculated by

$$\overline{\tau^2(t_n)} = \frac{\sum\limits_{\tau_m \in \mathcal{U}_n} P(\tau_m, t_n)\tau_m^2}{\sum\limits_{\tau_m \in \mathcal{U}_n} P(\tau_m, t_n)}, \quad (5)$$

and

$$\overline{\tau(t_n)} = \frac{\sum\limits_{\tau_m \in \mathcal{U}_n} P(\tau_m, t_n)\tau_m}{\sum\limits_{\tau_m \in \mathcal{U}_n} P(\tau_m, t_n)}. \quad (6)$$

In our measurement campaign, the signal sampling rate is 50 MHz, which results in the resolution of the delay domain is 20 ns.

TABLE II
STATISTICS OF PATH NUMBER IN THE U-SHAPE CUTTING SCENARIO.

Items	Path Number				
	Mean	S.D.	10%	50%	90%
CA	6	5	2	5	13
RA	9	4	4	8	14
WR	7	14	2	6	13
U-shape cutting in [8]	4	–	–	–	–

D. Doppler Spectrum

The doppler effect has significant influence on the fading rate of a particular propagation path, which indicates the level of the time selectivity of the channel. According to the definition, the doppler spectrum can be estimated by

$$D(\tau_m, \upsilon_n) = \mathscr{F}\{\, \mathscr{C}_n[\, h(\tau_m, t_n)\,]\,\}, \tau_m \in \mathcal{U}_n, \quad (7)$$

where $\mathscr{F}\{\cdot\}$ is the fast Fourier transformation. $\mathscr{C}_n[\,\cdot\,]$ is the correlation operation over t_n [5]. For the line-of-sight (LOS) case, it is assumed that the LOS propagation path is the first path of the extremum power value. And a correlation operation of 256 snapshot length with a channel sampling rate of 1968.504 Hz is employed in the following analysis, which results in a doppler frequency resolution of 15.34 Hz.

IV. Results and Analysis

A. Path Number

The statistics of the path number in CA, RA and WR are listed in Tab. II. The mean value of the path number in CA is a little larger than that in RA. The propagation condition in CA is not obstructed by the overpass as that in RA. So the signal may experience much more scattering and reflection to reach the RX in RA, which results in more paths can be extracted in RA. It should also be noted that the mean value of the path number in WR is 7, which is larger than the value 4 reported in [8]. The bandwidth of the measurement system settings in [8] is 3.84 MHz, which is much more narrow than that in our measurement, so that the delay resolution in our measurement is much higher. It may lead to the difference between our results and the results in [8].

The probability density distributions of the path number in CA and RA in the U-shape cutting scenario are illustrated in Fig. 4 and 5, respectively. The Gamma distribution is used to fit the probability density distribution of the path number. The probability density function of Gamma distribution is written as

$$f(x) = \frac{1}{\beta^\alpha \Gamma(\alpha)} x^{\alpha-1} e^{-\frac{x}{\beta}}, \qquad 0 \leqslant x \leqslant \infty, \quad (8)$$

where α and β are the shape and the scale parameters of the Gamma distribution, respectively. $\Gamma(\cdot)$ denotes the Gamma function.

As shown in Fig. 4 and 5, Gamma distributions fit the path number data well both in CA and RA. And the fitting α and β of the path number in CA are 2.14 and 2.92, whereas the fitting α and β in RA are 4.6 and 1.83.

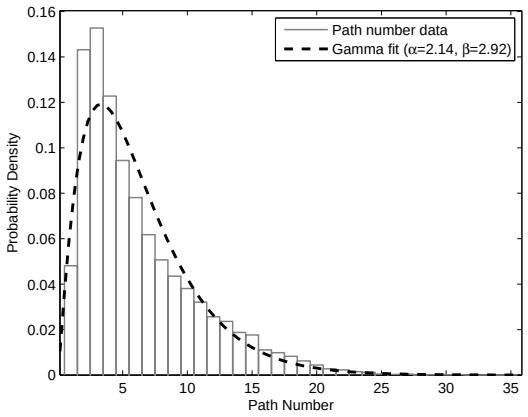

Fig. 4. PDF of path number in CA with a Gamma fit (the dash line).

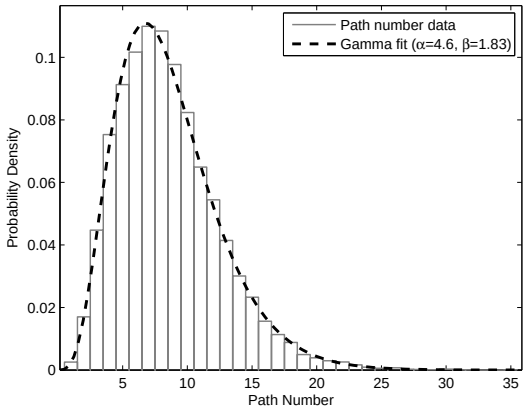

Fig. 5. PDF of path number in RA with a Gamma fit (the dash line).

B. Delay Spread

The probability density distributions of the rms DS in CA and RA are shown in Fig. 6 and 7. Both are fitted well by the Log-normal distribution. The fitting parameters $\mu(\log_{10}(s))$ and $\sigma(\log_{10}(s))$ of the rms DS in CA are -7.31 and 0.39, whereas those in RA are -6.71 and 0.40.

The statistics of rms DS in CA, RA and WR are all listed in Tab. III. On comparing the rms DS statistics in our measurement and in rural macro (RMa) scenario [11], we found that the rms DS reuslts in our measurement are quite different from the RMa scenario of the traditional cellular communication network. It accounts for that we can not use the channel parameters in traditional cellular communication network to simulate the HSR channel. From the table, it can be also found that the statistics of rms DS in our measurement are all larger than those in the D2a-fast train scenario presented in [3]. The propagation environment in D2a-fast train scenario is different from the U-shape cutting, so that it results in the difference in the statistics of rms DS in those two scenario. The similar difference is also presented in [8] where the rms DS in the U-shape cutting is larger than those in other scenarios

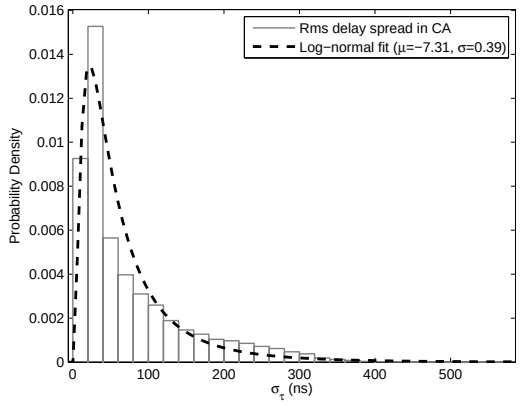

Fig. 6. PDF of rms DS in CA with a Log-normal fit (the dash line).

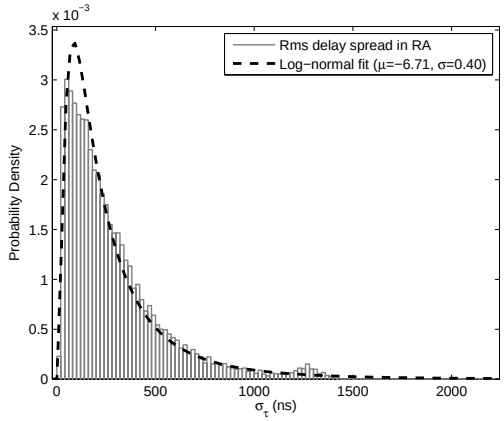

Fig. 7. PDF of rms DS in RA with a Log-normal fit (the dash line).

TABLE III
STATISTICS OF RMS DS IN THE U-SHAPE CUTTING SCENARIO.

Items	$\sigma_\tau(ns)$				
	Mean	S.D.	10%	50%	95%
CA	75	74	17	41	239
RA	286	257	53	210	813
WR	157	197	20	88	542
U-shape cutting [8]	–	–	–	–	800
D2a-fast train [3]	40	55	21	39	65
RMa (LOS) [11]	45	46	–	–	–

like plain and hill terrain. In addition, it is obvious that the mean value of the rms DS in CA is much smaller than that in RA. Thereby, it can be roughly inferred that the rms DS increases with the T-R distance.

In the sequel, Fig. 8 shows the growth of the rms DS with the T-R distance. Assuming that the rms DS is 0 ns at 0 m, we model the tendency of the rms DS against the T-R distance with a simple linear formula. The fitting linear formula is written as

$$\sigma_\tau(d) = 0.46 \cdot d, \qquad d \geqslant 0, \tag{9}$$

where d indicates the T-R distance. Equation 9 accounts for that the rms DS increases averagely 46 ns with the T-R

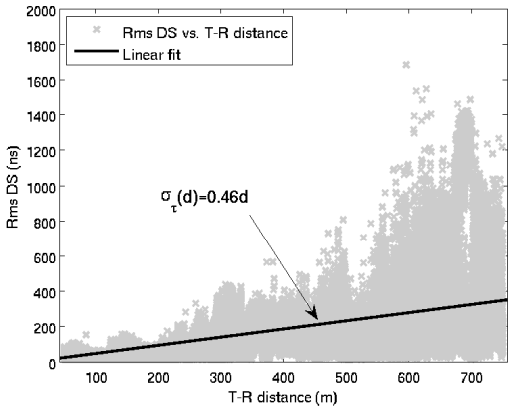

Fig. 8. Rms DS vs. T-R distance.

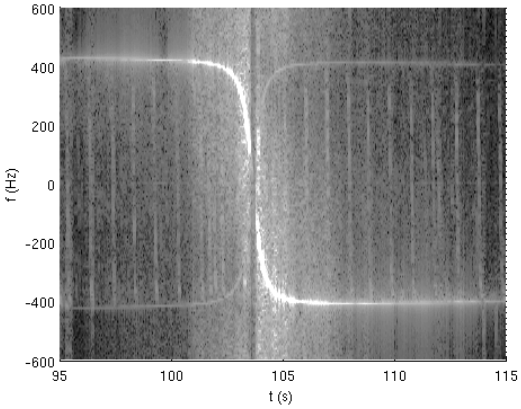

Fig. 9. Doppler spectrum in the U-shaping cutting scenario.

distance increasing 100 m in the U-shape cutting. Also, we can find the fluctuation around the fitting line is growing with the T-R distance from Fig. 8.

C. Doppler Spectrum

The theoretical doppler shift of the LOS path $f_{\mathrm{D}}(t)$ can be expressed as

$$f_{\mathrm{D}}(t) = \frac{v}{\lambda}\cos(\theta(t)), \qquad \lambda > 0 \quad and \quad v > 0, \tag{10}$$

where λ is the wavelength and v is the speed of the relative movement. $\theta(t)$ is the varying angle between the direction of the coming radio wave and the direction of the movement. So the doppler shift varies from a positive value to a negative value when the RX moves past the fixed TX.

The tendency of the doppler shift variation is demonstrated in our measurement, as illustrated in Fig. 9. The doppler spectrum curve shown as a "Z" shape in the figure sweeps from the positive maximum frequency shift to the negative maximum frequency shift as the train travels past the TX from the west to the east. It should be pointed out that two explicit curves are observed in the figure due to the symmetry of the doppler calculation method. In addition, the doppler spectrum curve breaks near the zero doppler frequency shift due to the severe loss of the receiving signals caused by the obstruction of the overpass near the TX location. The maximum doppler frequency shift in the U-shape cutting scenario is 428 Hz. So the corresponding speed of the traveling train is 196 km/h, which is close to the realistic speed during the measurement.

V. Conclusion

In this paper, small scale fading characteristics including path number, rms DS, and doppler frequency shift, are analyzed on the basis of the wideband HSR channel measurement at a center frequency of 2.35 GHz with 50 MHz bandwidth in the U-shape cutting scenario of Zhengzhou–Xian HSR line in China. The measurement route is divided into two parts named as CA and RA corresponding to the close and remote T-R distance ranges, respectively. The distributions of the path number both in CA and RA are fitted well by the Gamma distribution whereas the Log-normal distribution fits the rms DS well. The statistics of rms DS are quite different from those in RMa scenario and other HSR scenarios. Also, the mean value of the rms DS in CA is 75 ns, which is obviously smaller than 286 ns in RA. On the basis of the difference of the mean values of the rms DS in CA and RA, a linear fit is used to model the increasing tendency of rms DS against the T-R distance. Finally, the LOS path doppler shift is analyzed and is found to meet the theoretical value precisely.

Acknowledgment

The research is supported by National Key Technology Research and Development Program of the Ministry of Science and Technology of China (NO. 2012BAF14B01), and National Science and Technology Major Project of the Ministry of Science and Technology (NO. 2012ZX03001030-004), and National Natural Science Foundation of China (NO. 61171105), and Program for New Century Excellent Talents in University of Ministry of Education of China (NCET-11-0598). Also, the authors also would like to thank the great help of the colleges of Beijing Jiaotong University and China Academy of Railway Sciences.

References

[1] H. Wei, Z. Zhong, K. Guan, and B. Ai, "Path loss models in viaduct and plain scenarios of the high-speed railway," in *Proc. 5th Int Communications and Networking in China (CHINACOM) ICST Conf*, 2010, pp. 1–5.

[2] R. He, Z. Zhong, B. Ai, and J. Ding, "Propagation measurements and analysis for high-speed railway cutting scenario," *Electronics Letters*, vol. 47, no. 21, pp. 1167–1168, 2011.

[3] *WINNER II Channel Models*, IST-WINNER II Deliverable 1.1.2, 2008.

[4] *Propsound multidimensional channel sounder, Elektrobit Ltd. [Online]. Available: http://www.propsim.com*.

[5] L. Liu, C. Tao, J. Qiu, H. Chen, L. Yu, W. Dong, and Y. Yuan, "Position-based modeling for wireless channel on high-speed railway under a viaduct at 2.35 ghz," *IEEE Journal on Selected Areas in Communications*, vol. 30, no. 4, pp. 834–845, 2012.

[6] R.Parviainen and K. Pekka, "Results of high speed train channel measurements," *European Cooperation in the Field of Scientific and Technical Research*, 2008.

[7] J. Lu, G. Zhu, and C. Briso-Rodriguez, "Fading characteristics in the railway terrain cuttings," in *Proc. IEEE 73rd Vehicular Technology Conf. (VTC Spring)*, 2011, pp. 1–5.

[8] J. Qiu, C. Tao, L. Liu, and Z. Tan, "Broadband channel measurement for the high-speed railway based on wcdma," in *Proc. IEEE 75th Vehicular Technology Conf. (VTC Spring)*, 2012, pp. 1–5.
[9] "Sencity rail antenna: 1399.17.0039 huber+suhner data sheet," *HUBER+SUHNER AG RF Industrial*, 2010.
[10] T. S. Rappaport, *Wireless Communications: Principles and Practice*. PrenticeHall, New Jersey, 1996.
[11] *Guidelines for Evaluation of Radio Interface Technologies for IMT-Advanced*, ITU-R Report M.2135, Nov. 2008.